

A Quick Introduction to Seismic Imaging

Alison Malcolm

Memorial University of Newfoundland

September 12, 2017

A Sense of Scale

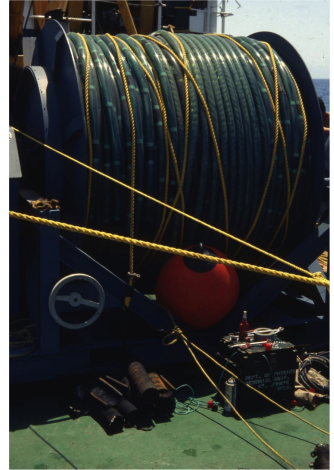
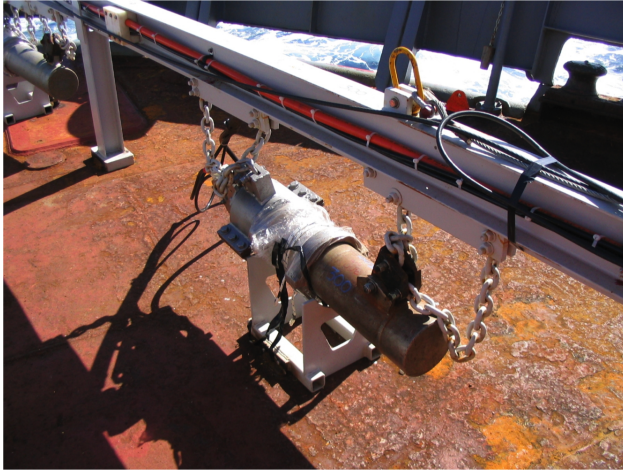


Terrabytes of data!

Images from: <http://www.offshoreenergytoday.com/pgs-seismic-vessel-transfers-data-to-shore-via-12-mbits-link/> and

<https://www.pgs.com/marine-acquisition/tools-and-techniques/the-fleet/flexible-capacity/sanco-sword/>

Data Acquisition



Images courtesy Prof. Jeremy Hall

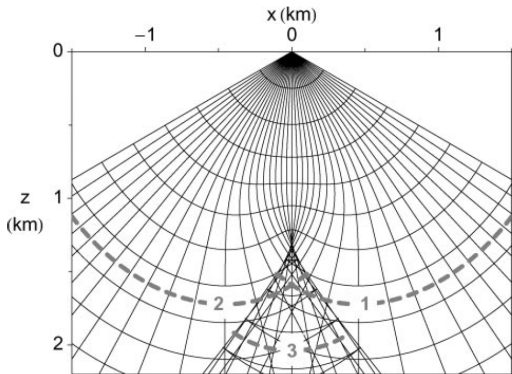
Schematic View of Wave Propagation

(measurement movie)

From: <https://giphy.com/gifs/refraction-pbGzTWOkabGFy/download>

Why is this hard?

material	$c(x)$
sedimentary rocks:	2-4 km/s
igneous rocks:	2-7 km/s
metamorphic rocks:	1-4 km/s
at depth:	8-10 km/s



Stolk & Symes (2004)

travel distance: tens of wavelengths

Mathematical Model

e.g. Achenbach (73), Landau & Lifshitz (86), Aki & Richards (02)

Conservation of momentum ($F = ma$):

$$\rho \frac{Dv_j}{Dt} = \rho f_j + \partial_i \sigma_{ij}$$

$$\frac{Da}{Dt} = \frac{\partial a}{\partial t} + \mathbf{v} \cdot \nabla \mathbf{a}$$

Hooke's Law (linearly elastic, isotropic material):

$$\sigma_{ij} = \lambda \epsilon_{kk} \delta_{ij} + 2\mu \epsilon_{ij}$$

σ_{ij} stress tensor

$\epsilon_{ij} = \frac{1}{2} \left(\frac{\partial u_i}{\partial x_j} + \frac{\partial u_j}{\partial x_i} \right)$ strain tensor

Mathematical Model

General Assumptions:

- long wavelength compared to amplitude
- smooth displacement

For Today:

- linear elasticity
- constant density
- isotropy

Mathematical Model

Elastic Wave Equation:

$$\rho \frac{\partial^2 u_j}{\partial t^2} = (\lambda + \mu) \partial_j \partial_k u_k + \mu \nabla^2 u_j$$

Mathematical Model

Elastic Wave Equation:

$$\rho \frac{\partial^2 u_j}{\partial t^2} = (\lambda + \mu) \partial_j \partial_k u_k + \mu \nabla^2 u_j$$

Helmholtz decomposition: $\mathbf{u} = \nabla \phi + \nabla \times \psi$

Mathematical Model

Elastic Wave Equation:

$$\rho \frac{\partial^2 u_j}{\partial t^2} = (\lambda + \mu) \partial_j \partial_k u_k + \mu \nabla^2 u_j$$

Helmholtz decomposition: $\mathbf{u} = \nabla \phi + \nabla \times \psi$

$$\partial_t^2 \phi = c_p^2 \nabla^2 \phi$$

$$\partial_t^2 \psi = c_s^2 \nabla^2 \psi$$

See Aki & Richards 2002 book

$$c_p = \sqrt{(\lambda + 2\mu)/\rho}$$
$$c_s = \sqrt{\mu/\rho}$$

Acoustic Simplification

Acoustic (really P-wave only) assumption

$$\nabla^2 \phi - \frac{1}{c^2} \partial_t^2 \phi = f$$

$$\phi = 0 \quad t < 0$$

$$\partial_z \phi|_{z=0} = 0$$

Reasons:

- sources and receivers often in the ocean
- computational cost

Contrast Formulation

Acoustic (really P-wave only) assumption

$$\mathbf{L}\phi := \nabla^2 \phi - \frac{1}{c^2} \partial_t^2 \phi = \mathbf{f}$$

Linearize: $\mathbf{c}(\mathbf{x}) = \mathbf{c}_0(\mathbf{x}) + \delta \mathbf{c}(\mathbf{x})$

$$\mathbf{L}\phi = \mathbf{f}$$

$$\mathbf{L}_0 \phi_0 = \mathbf{f}$$

note that \mathbf{L}_0 and ϕ_0 use $\mathbf{c}_0(\mathbf{x})$

Contrast Formulation

Acoustic (really P-wave only) assumption

$$\mathbf{L}\phi := \nabla^2 \phi - \frac{1}{c^2} \partial_t^2 \phi = \mathbf{f}$$

Linearize: $\mathbf{c}(\mathbf{x}) = \mathbf{c}_0(\mathbf{x}) + \delta \mathbf{c}(\mathbf{x})$

$$\mathbf{L}\phi = \mathbf{f}$$

$$\mathbf{L}_0 \phi_0 = \mathbf{f}$$

note that \mathbf{L}_0 and ϕ_0 use $\mathbf{c}_0(\mathbf{x})$

subtract

$$\mathbf{L}_0 \delta \phi = \delta \mathbf{L} \phi$$

Symes 09 and Stolk 00 give estimates on linearization error

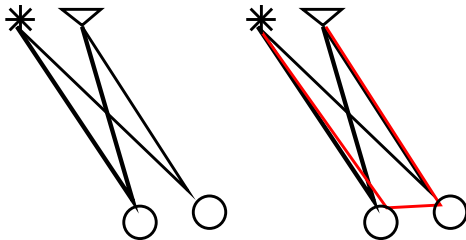
Contrast formulation

Born approximation

$$\mathbf{L}_0 \delta \phi = \delta \mathbf{L} \phi_0$$

$$\nabla^2 \delta \phi - \frac{1}{c_0^2} \partial_t^2 \delta \phi = \frac{2\delta c}{c_0^3} \partial_t^2 \phi_0$$

$\delta \phi$ is called the scattered field

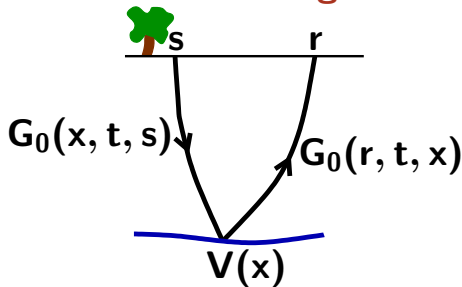


Separation of Scales

$$\nabla^2 \delta\phi - \frac{1}{c_0^2} \partial_t^2 \delta\phi = \frac{2\delta c}{c_0^3} \partial_t^2 \phi_0$$

We assume that **on the scale of the wavelength:**

- δc is oscillatory
- c_0 is smooth

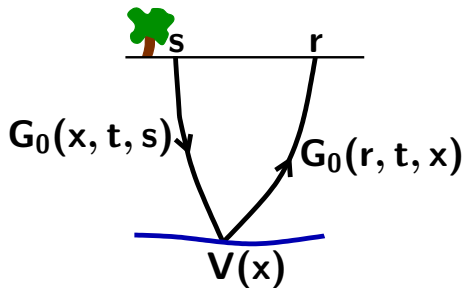


Data Model

$$\nabla^2 \delta\phi - \frac{1}{c_0^2} \partial_t^2 \delta\phi = \frac{2\delta c}{c_0^3} \partial_t^2 \phi_0$$

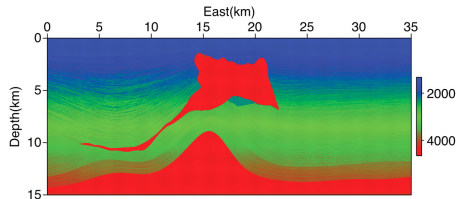
Assume a δ -source

$$\delta\phi(s, r, \omega) = - \int_x \mathbf{G}_0(r, \omega, x) \underbrace{\frac{2\delta c(x)}{c_0(x)^3}}_{V(x)} \omega^2 \mathbf{G}_0(x, \omega, s) dx$$

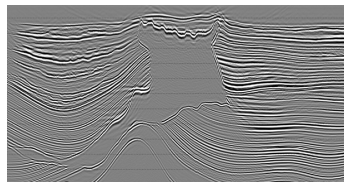


'Typical' Processing Steps

- 1 Filtering/Signal Processing/Geometry/Statics
(we will ignore these steps)
- 2 Velocity analysis, i.e. find c_0 ,
usually via iterative imaging
- 3 Imaging (a.k.a. Migration),
i.e. find δc



Model Velocity (m/s) for North=20 km



From: Fehler & Larner TLE, 2008, <http://tle.geoscienceworld.org/content/27/8/1006> and Spectrum

<http://www.spectrumgeo.com/imaging-services/land-environment/depth-processing/pre-stack-depth-migration>

Imaging Methods

Increasing complexity \Rightarrow

- 1 Stacking (aka averaging)
- 2 Kirchhoff Migration
- 3 One-way methods
- 4 Reverse-time methods

Velocity Analysis Methods

Increasing complexity \Rightarrow

- 1 Normal Moveout Analysis/Semblance
- 2 Iterative Kirchhoff Migration
- 3 Iterative One-way methods
- 4 Iterative Reverse-time methods
–Full-Waveform Inversion (FWI)

Ray Tracing

(very briefly)

Assume solution form:

$$\phi_0(\mathbf{x}, t) = e^{i\omega\psi(\mathbf{x},t)} \sum_k \frac{A_k(\mathbf{x}, t)}{(i\omega)^k}$$

- A_k , and ψ SMOOTH
- $e^{i\omega\psi(\mathbf{x},t)}$ oscillatory
- remove frequency dependence

Developed by Wentzel, Kramers, Brillouin, independently in 1926 and by Jeffreys in 1923;
see Appendix E of Bleistein, Cohen and Stockwell for more details.

Ray Tracing

(very briefly)

Apply Helmholtz to

$$\phi_0(\mathbf{x}, t) = e^{i\omega\psi(\mathbf{x}, t)} \sum_{\mathbf{k}} \frac{\mathbf{A}_{\mathbf{k}}(\mathbf{x}, t)}{(i\omega)^k}$$

Eikonal equation:

$$(\nabla\psi)^2 = \frac{1}{c(\mathbf{x})^2}$$

Transport equations:

$$2\nabla\psi \cdot \mathbf{A}_{\mathbf{k}} + \mathbf{A}_{\mathbf{k}} \nabla^2\psi = 0$$

Ray Tracing

(very briefly)

Eikonal equation:

$$(\nabla\psi)^2 = \frac{1}{c(x)^2}$$

Transport equations:

$$2\nabla\psi \cdot \mathbf{A}_k + \mathbf{A}_k \nabla^2\psi = 0$$

- 1 **Nonlinear!**
- 2 Method of characteristics (ray-tracing)
- 3 Usually use Runge-Kutta (requires smooth c)
- 4 Note that for constant velocity rays are straight lines

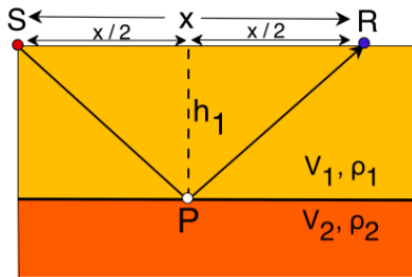
Simplest Approach

Stacking and Normal-Moveout Analysis

$$t(x) = \frac{2}{c} \sqrt{h_1^2 + \left(\frac{x}{2}\right)^2}$$

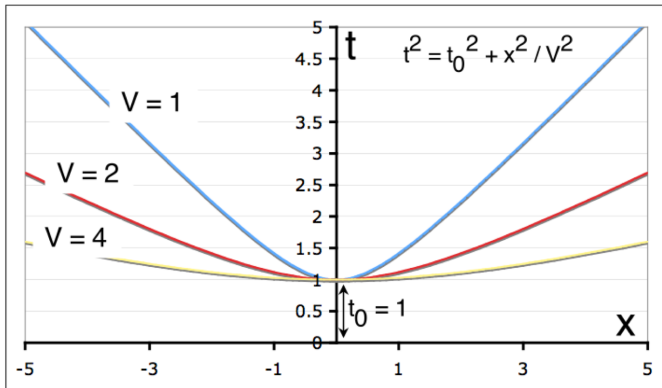
Correct for the x-dependence

$$t^{\text{corr}}(x) = t^{\text{meas}}(x) - \frac{2}{c} \sqrt{\left(\frac{x}{2}\right)^2 + \left(\frac{t(0)}{2}\right)^2}$$



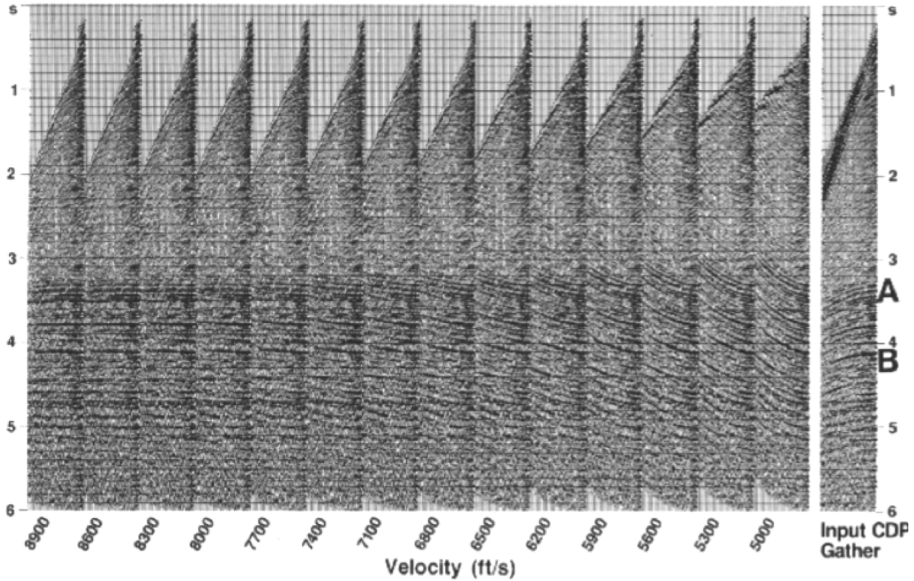
This is called the **Normal Moveout Correction (NMO)**.

NMO Velocity Analysis

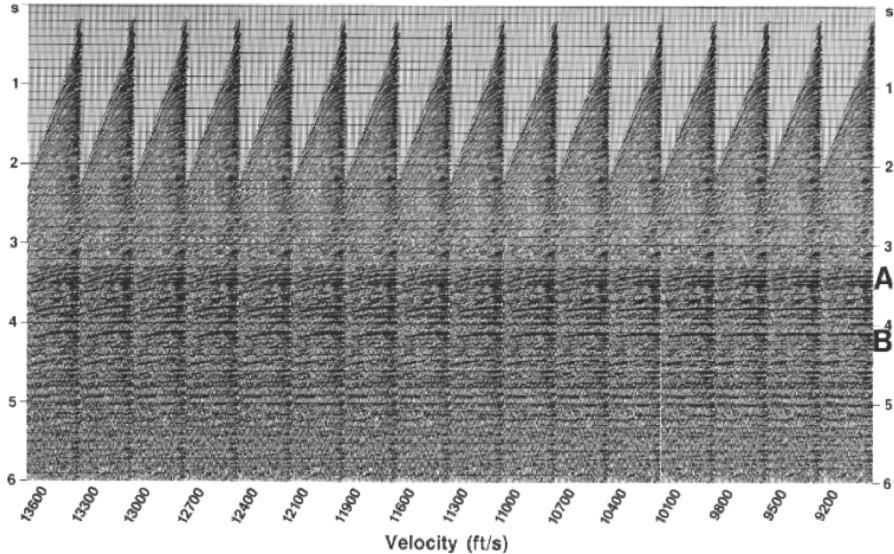


Minimizing $\partial_x t(x) = 0$ gives a measure of velocity.

NMO Velocity Analysis



NMO Velocity Analysis



A more refined method

Differential Semblance

Minimize:

$$J_h = \frac{1}{2} \int h^2 I^2(x, z, h) dx dz dh$$

where $I(x, z, h)$ is the NMO-corrected data before stacking (averaging).

DSO (Differential Semblance Optimization) has been extensively studied by Symes and co-authors. Of particular importance are Santosa & Symes (1986) and Shen & Symes (2008)

Kirchhoff Migration

WKBJ Modeling

$$\delta\phi(s, r, t) = \int_{\mathbf{x}} \int_{\mathbf{T}} \mathbf{G}_0(r, t - t_0, \mathbf{x}) \frac{2\delta c(\mathbf{x})}{c_0(\mathbf{x})^2} \partial_t^2 \mathbf{G}_0(\mathbf{x}, t_0, s) d\mathbf{x} dt_0$$

$$\mathbf{G}_0(\mathbf{x}, t_0, s) \approx \int \mathbf{A}(\mathbf{x}, s, \omega) e^{i\omega(t - T(\mathbf{x}, s))} d\omega$$

$$\delta\phi(s, r, t) = \int_{\mathbf{x}} \int_{\mathbb{R}} \omega^2 \overbrace{\mathbf{A}(\mathbf{x}, s, \omega) \mathbf{A}(r, \mathbf{x}, \omega)}^{B(\mathbf{x}, r, s, \omega)} \frac{2\delta c(\mathbf{x})}{c_0(\mathbf{x})^2} e^{i\omega(t - T(s, \mathbf{x}) - T(\mathbf{x}, r))} d\mathbf{x} d\omega$$

Kirchhoff Migration

WKBJ Modeling Formula

$$\delta\phi(\mathbf{s}, \mathbf{r}, t) = \int_{\mathbf{x}} \int_{\mathbb{R}} \omega^2 \mathbf{B}(\mathbf{x}, \mathbf{r}, \mathbf{s}, \omega) e^{i\omega(t - T(\mathbf{s}, \mathbf{x}) - T(\mathbf{x}, \mathbf{r}))} d\mathbf{x} d\omega$$

Assume \mathbf{B} independent of ω

$$\delta\phi(\mathbf{s}, \mathbf{r}, t) = \int_{\mathbf{x}} \mathbf{B}(\mathbf{x}, \mathbf{r}, \mathbf{s}) \delta''(t - T(\mathbf{s}, \mathbf{x}) - T(\mathbf{x}, \mathbf{r})) d\mathbf{x}$$

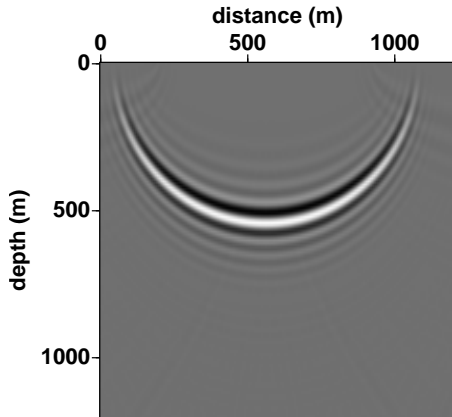
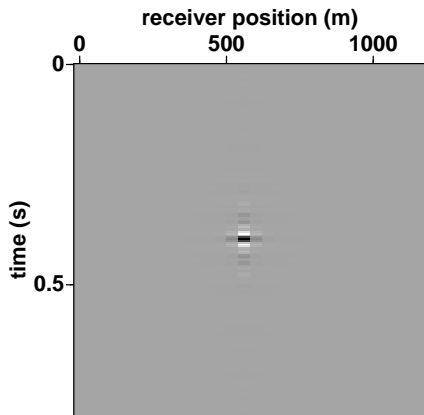
This is a **Generalized Radon Transform**

Note that a Radon transform is often called a τ -p transform in exploration seismology.

Kirchhoff Migration

WKBJ Modeling Formula

$$\delta\phi(s, r, t) = \int_{\mathbf{x}} \mathbf{B}(\mathbf{x}, r, s) \delta''(t - \mathbf{T}(s, \mathbf{x}) - \mathbf{T}(\mathbf{x}, r)) d\mathbf{x}$$



Kirchhoff Migration

Goal: Locate the singularities of δc from $\delta\phi$

Requires \mathbf{F}^{-1}

Recall: data are redundant

Least Squares: $\mathbf{F}_{LS}^{-1} = (\mathbf{F}^* \mathbf{F})^{-1} \mathbf{F}^*$

$$\mathbf{F}^*[\delta\phi](\mathbf{x}) = \int_{\mathbf{R}} \int_{\mathbf{S}} \int_{\mathbb{R}^{2n-1}} \omega^2 \overline{\mathbf{B}(\mathbf{x}, \mathbf{r}, \mathbf{s}, \theta)} e^{-i\omega(t - \mathbf{T}(\mathbf{s}, \mathbf{x}) - \mathbf{T}(\mathbf{x}, \mathbf{r}))} d\theta d\mathbf{s} d\mathbf{r}$$

(Beylkin (85), Rakesh (88), Symes (95))

Velocity Analysis: Kirchhoff Methods

Data are redundant, exploit the redundancy to find the velocity model $c(x) \mapsto c(x, h)$, we find

$$\underset{c}{\operatorname{argmin}}(\partial_h F^*[c](d(s, r, t)))$$

h can be

- offset (almost NMO)
- **scattering angle**
- subsurface offset
- time
- ...

Symes' 2009 review paper has an overview of this Symes 1999, 2001 justifies the use of local optimization for layered partially linearized inversions

Imaging Methods – Summary

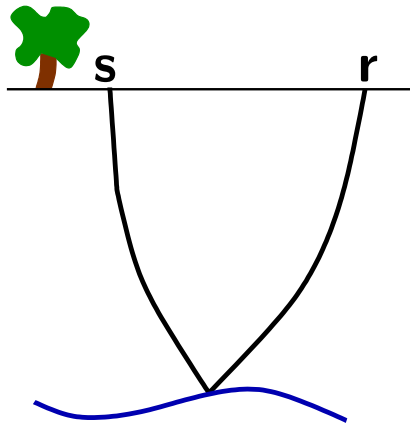
- Kirchhoff
 - ▶ Integral technique, **usually** uses ray theory
 - ▶ Linearized with Kirchhoff approximation
 - ▶ Related to X-ray CT imaging
 - ▶ Generalized Radon Transform
- For velocity analysis, iterate over ‘flatness’

One-Way Methods

Physical Motivation

- downward continuation
- imaging condition

Claerbout 71, 85



One-Way Methods

Approximating the Wave Equation

Idea (1D, c constant=1):

$$(\partial_x^2 - \partial_t^2)\phi = (\partial_x - \partial_t)(\partial_x + \partial_t)\phi$$

c not constant:

$$(c(x)^2 \partial_x^2 - \partial_t^2)\phi = (c(x)\partial_x - \partial_t)(c(x)\partial_x + \partial_t)\phi - c(x)(\partial_x c(x))\partial_x \phi$$

$c(x)$ smooth \Rightarrow better approximation

Taylor (81), Stolk & de Hoop (05) give more detail and more dimensions

Imaging Methods – Summary

- Kirchhoff
 - ▶ Integral technique, **usually** uses ray theory
 - ▶ Linearized with Kirchhoff approximation
 - ▶ Related to X-ray CT imaging
 - ▶ Generalized Radon Transform
- One-way
 - ▶ Based on a paraxial approximation
 - ▶ Usually computed with finite differences
- For velocity analysis, iterate over ‘flatness’

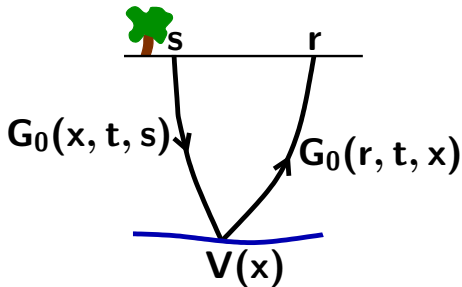
Reverse-Time Migration

Forming an Image

Procedure:

Whitmore (83), Loewenthal & Mufti (83), Baysal et al (83)

- back propagate in time
- imaging condition



Reverse-Time Migration

an Adjoint State Method

Lailly (83,84), Tarantola (84,86,87) Symes (09)

For a fixed source, s,

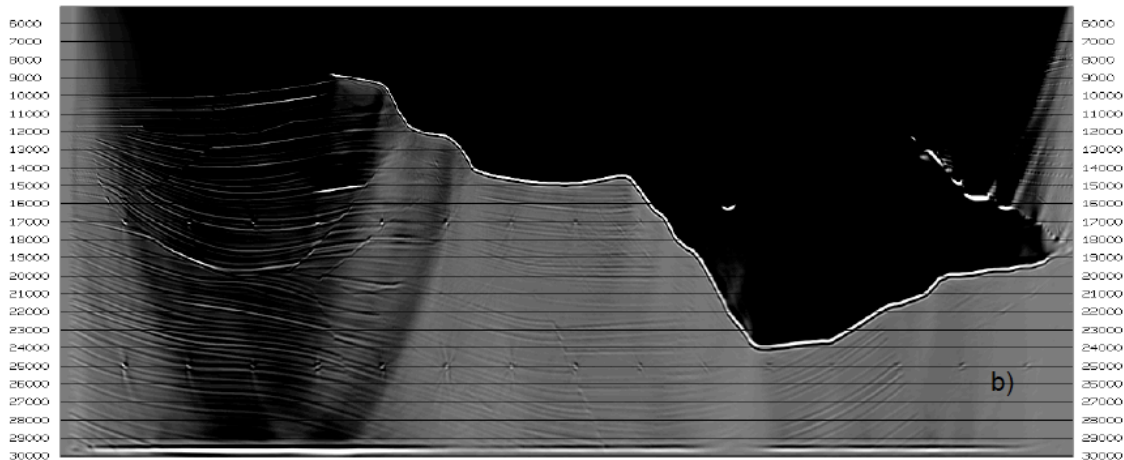
$$(c^{-2}\partial_t^2 - \nabla^2)q(x, t; s) = \int_{R_s} \delta\phi(r, t; s)\delta(x - r)dr$$
$$q(\cdot, t, \cdot) = 0 \text{ for } t > T$$

receivers act as sources, reversed in time

$$Im(x) = \frac{2}{c^2(x)} \int \int q(x, t; s) \partial_t^2 G_0(x, t, s) dt ds$$

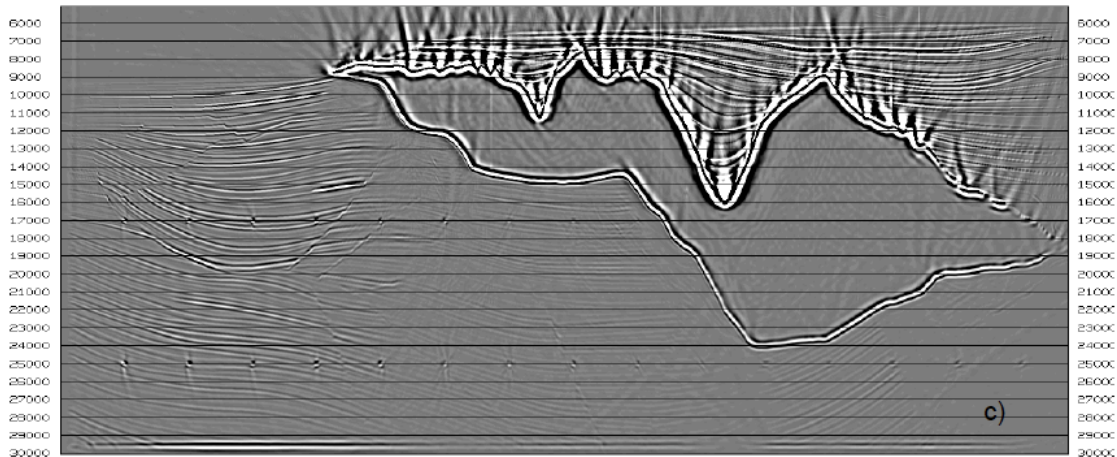
Reverse-Time Migration

Example Liu et al (07)



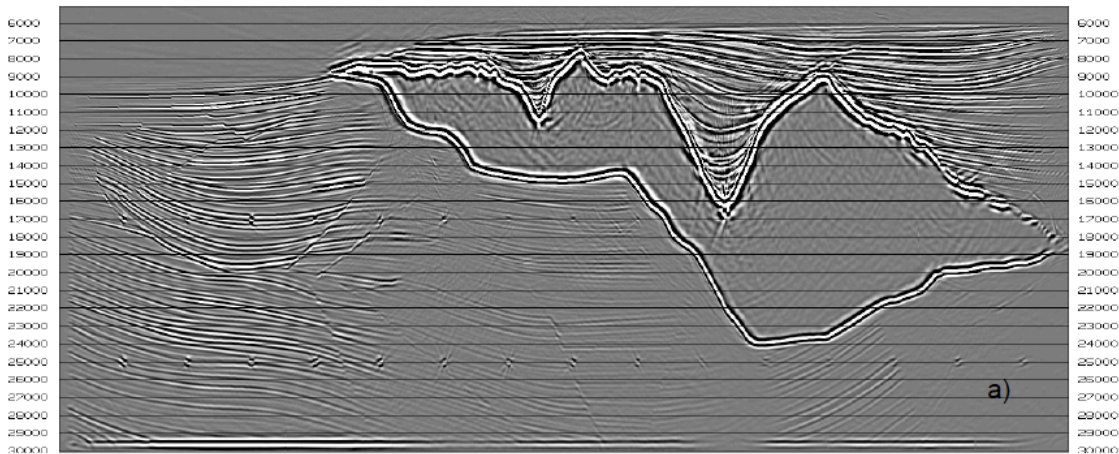
Reverse-Time Migration

Example Liu et al (07)



Reverse-Time Migration

Example Liu et al (07)



Imaging Methods – Summary

- Kirchhoff

- ▶ Integral technique, **usually** uses ray theory
- ▶ Linearized with Kirchhoff approximation
- ▶ Related to X-ray CT imaging
- ▶ Generalized Radon Transform

- One-way

- ▶ Based on a paraxial approximation
- ▶ Usually computed with finite differences

- Reverse-time migration (RTM)

- ▶ Run wave-equation backward
- ▶ Usually computed with finite differences
- ▶ “No” approximations (to the acoustic, linearized wave-equation, for smooth media assuming no multiple scattering)

Full-Waveform Inversion

Recall our initial formulation:

$$\mathbf{L}\phi := (\nabla^2 - \frac{1}{c^2}\partial_t^2)\phi = \mathbf{f}$$

$$\mathbf{L}\mathbf{G} = \delta$$

$$\mathbf{u} = 0 \quad \mathbf{t} < 0$$

$$\partial_z \mathbf{u}|_{z=0} = 0$$

FWI attempts to solve for c directly given \mathbf{u}, \mathbf{f}

there is no **explicit** splitting of c , but a smooth approximation is generally obtained

Full-Waveform Inversion

Recall our initial formulation:

$$\mathbf{L}\phi := (\nabla^2 - \frac{1}{c^2}\partial_t^2)\phi = \mathbf{f}$$

$$\mathbf{L}\mathbf{G} = \delta$$

Define

$$\mathcal{J} = \|\mathbf{G} - \mathbf{d}\|_{L^2((S,R)\times[0,T])}^2$$

Find c that minimizes \mathcal{J}

L_2 is perhaps not the ideal norm (e.g. Symes (10))

Some references: Fichtner (book), 2011, Tarantola, (1987), Virieux & Operto (2009)

Full-Waveform Inversion

The Optimization Problem

$$\mathcal{J} = \|\mathbf{G} - \mathbf{d}\|_{L^2((S,R) \times [0,T])}^2$$

Find $\delta\mathbf{m}$ s.t. $\mathcal{J}(\mathbf{m}_0 + \delta\mathbf{m}) < \mathcal{J}(\mathbf{m}_0)$

Full-Waveform Inversion

The Optimization Problem

$$\mathcal{J} = \|\mathbf{G} - \mathbf{d}\|_{L^2((S,R) \times [0,T])}^2$$

Find δm s.t. $\mathcal{J}(m_0 + \delta m) < \mathcal{J}(m_0)$

$$\mathcal{J}(m) \approx \mathcal{J}(m_0) + \frac{\partial \mathcal{J}}{\partial m_0}(m_0) \delta m$$

in continuous form

$$\mathcal{J}(m(x)) \approx \mathcal{J}(m_0(x)) + \int \frac{\partial \mathcal{J}}{\partial m_0}(x') \delta m(x') dx'$$

m can be c , c^{-1} , c^{-2} etc

Full-Waveform Inversion

The Optimization Problem

$$\mathcal{J}(\mathbf{m}(\mathbf{x})) \approx \mathcal{J}(\mathbf{m}_0(\mathbf{x})) + \int \frac{\partial \mathcal{J}}{\partial \mathbf{m}_0(\mathbf{x}')} \delta \mathbf{m}(\mathbf{x}') d\mathbf{x}'$$

Find the minimum, set $\frac{\partial \mathcal{J}}{\partial \mathbf{m}_0} = 0$

$$\begin{aligned} \left. \frac{\partial \mathcal{J}}{\partial \mathbf{m}_0(\mathbf{x})} \right|_{\mathbf{m}} &\approx \left. \frac{\partial \mathcal{J}}{\partial \mathbf{m}_0(\mathbf{x})} \right|_{\mathbf{m}_0} + \int \frac{\partial^2 \mathcal{J}}{\partial \mathbf{m}_0(\mathbf{x}) \partial \mathbf{m}_0(\mathbf{x}')} \delta \mathbf{m}(\mathbf{x}') d\mathbf{x}' \\ &= \mathbf{g}(\mathbf{m}_0; \mathbf{x}) + \int \mathbf{h}(\mathbf{m}_0; \mathbf{x}, \mathbf{x}') \delta \mathbf{m}(\mathbf{x}') d\mathbf{x}' \end{aligned}$$

g is the gradient and **h** is the hessian of \mathcal{J}

Full-Waveform Inversion

The Optimization Problem

$$= g(m_0; x) + \int h(m_0; x, x') \delta m(x') dx'$$

$$\delta m(x) \approx \int h^{-1}(m_0; x, x') g(m_0; x') dx'$$

g is the gradient and **h** is the hessian of \mathcal{J}

This derivation is based on Margrave, Yedlin & Innanen (2011), CREWES report

Full-Waveform Inversion

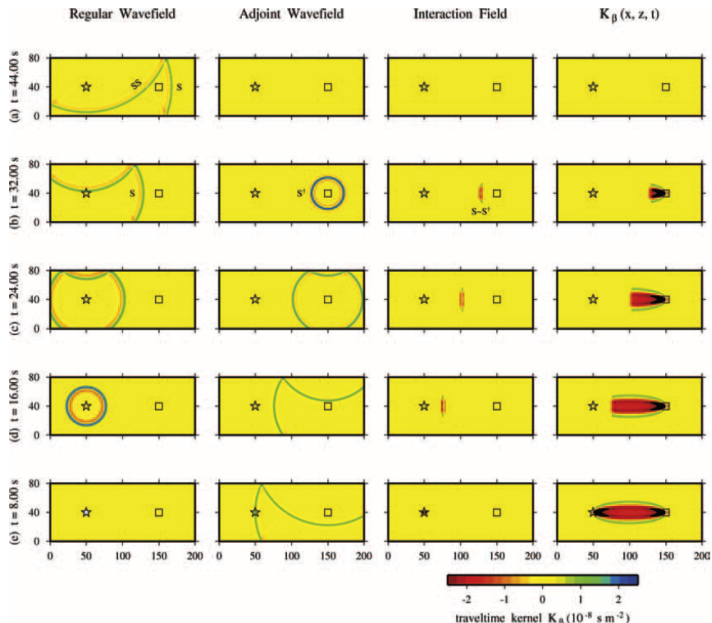
The Optimization Problem

$$\delta m(x) \approx \int h^{-1}(m_0; x, x') g(m_0; x') dx'$$

$$g(m_0; x) = \int_{\Omega, S, R} \underbrace{G_0(s, x)}_{\text{source}} \overbrace{[G_0(x, r) \delta d(s, r, \omega)]}^{\text{back-propagated data residual}} ds dr d\omega$$

This derivation is based on Margrave, Yedlin & Innanen (2011), CREWES report

Tromp et al (2005)



The Gradient and Hessian

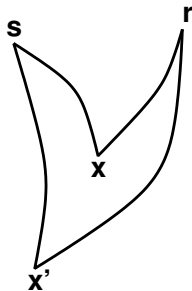
Summary

- $g(x)$ – size of model
xcorr:
 - backpropagated residuals
 - modeled source
 - cost: two propagation steps

The Gradient and Hessian

Summary

- $h(x, x') = h_1(x, x') + h_2(x, x')$
 - $(\text{model size})^2$
 - ▶ h_1 depends on δd
 - ▶ h_2 does not \Rightarrow dominates
 - h_2 has 4 propagation steps



See Fichtner's book [11] for an excellent overview of the physical meaning of the Hessian and its relationship to the covariance, and Metivier et al, 2013, 2014, [17, 15] for a more numerical-analysis-y overview.

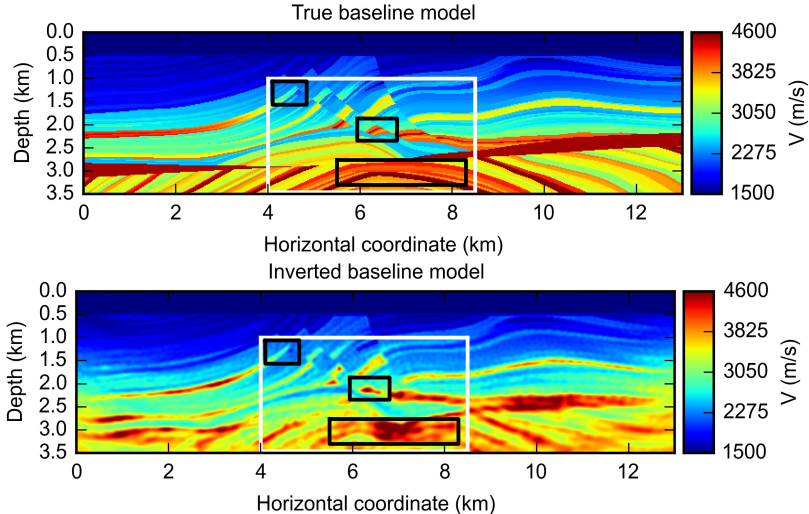
Key Issues

Full-Waveform Inversion

- **Computational Cost:** lots of Helmholtz or wave equation solves.
- **Non-convexity:** Initial model must be close to the true model for convergence.
- **Uncertainty Quantification:** How do we quantify the way errors in our data effect our final results and interpretations of both velocity models and the resulting images?

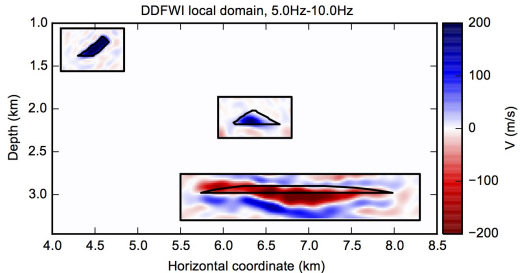
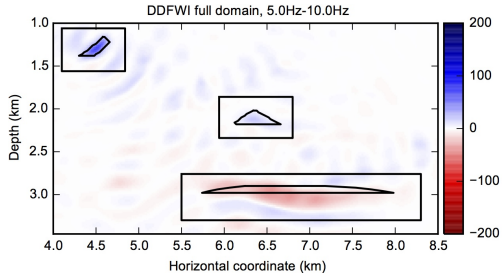
A local FWI solver

Willemsen & M (2016), M & Willemsen (2016)



A local FWI solver

Willemsen & M (2016), M & Willemsen (2016)



- Much faster than solving in the full domain
- Reduced model space also improves convergence
- 3D is still a challenge

Key Recent Developments

Full-Waveform Inversion

Up to 2009 is well summarized by Virieux and Operto (2009) (which has been cited 1000 times since 2016)

- Different objective functions:[6],[3],[13],[16],[8]
- Multi-parameter: [4],[5],[18],[19],[12],[25]
- Extend or change the model/combine with tomography:[20],[2],[22],[1],[24],[7]
- Uncertainty Quantification: [14],[9],[26],[27]
- Lots of developments on the numerics of solving and updates, organizing data etc

General References

- Symes Review [21]
- Virieux Review [23]
- Etgen Review [10]
- Books:
 - ▶ Aki & Richards “Quantatative Seismology”
 - ▶ Oz Yilmazs “Seismic Data Analysis: Processing, Inversion, and Interpretation of Seismic Data”
 - ▶ Bleistein, Cohen and Stockwell “Mathematics of Multidimensional Seismic Imaging, migration and Inversion”
 - ▶ Stein & Wysession “Introduction to Seismology”

DD25: JULY 23-27, 2018

25TH INTERNATIONAL CONFERENCE ON DOMAIN DECOMPOSITION METHODS

ST. JOHN'S, NEWFOUNDLAND, CANADA



- Meeting will attract world's leading computational scientists, mathematicians, engineers interested in the parallel solution of PDEs
- 13 Plenary Speakers
- Tutorial style pre-conference short course
- Industrial geophysical problem minisymposia
- See dd25.math.mun.ca for more information



Tariq Alkhalifah and Yunseok Choi.

From tomography to full-waveform inversion with a single objective function.
GEOPHYSICS, 79(2), 2014.



Ali Almomin and Biondo Biondi.

Tomographic Full Waveform Inversion : Practical and Computationally Feasible Approach.
2012 SEG Technical Program Expanded Abstracts, pages 1–5, 2012.



Aleksandr Aravkin, Tristan Van Leeuwen, and Felix Herrmann.

Robust full-waveform inversion using the Student's t-distribution.
2011 SEG Technical Program Expanded Abstracts, pages 2669–2673, 2011.



Christophe Barnes and Marwan Charara.

The domain of applicability of acoustic full-waveform inversion for marine seismic data.
GEOPHYSICS, 74(6):WCC91–WCC103, November 2009.



Romain Brossier, Stéphane Operto, and Jean Virieux.

Seismic imaging of complex onshore structures by 2D elastic frequency-domain full-waveform inversion.
GEOPHYSICS, 74(6):WCC105–WCC118, November 2009.



Romain Brossier, Stéphane Operto, and Jean Virieux.

Which data residual norm for robust elastic frequency-domain full waveform inversion?
GEOPHYSICS, 75(3):R37–R46, May 2010.



Debanjan Datta and Mrinal K. Sen.

Estimating a starting model for full-waveform inversion using a global optimization method.
GEOPHYSICS, 81(4):R211–R223, 2016.



Laurent Demanet and Vincent Jugnon.

Convex recovery from interferometric measurements.
IEEE Transactions on Computational Imaging, 3(2):282–295, 2017.



Gregory Ely, Alison Malcolm, and David Nicholls.

Combining global optimization and boundary integral methods to robustly estimate subsurface velocity models.

In SEG Technical Program Expanded Abstracts 2015, pages 3729–3733. Society of Exploration Geophysicists, 2015.



John Etgen, Samuel H Gray, and Yu Zhang.

An overview of depth imaging in exploration geophysics.
Geophysics, 74(6):WCA5–WCA17, 2009.



Andreas Fichtner and Jeannot Trampert.

Resolution analysis in full waveform inversion.
Geophysical Journal International, 187(3):1604–1624, December 2011.



Kristopher A Innanen.

Seismic AVO and the inverse Hessian in pre-critical reflection full waveform inversion.
Geophysical Journal International, 199(2):717–734, 2014.



Rie Kamei, AJ Breeders, and RG Pratt.

A discussion on the advantages of phase-only waveform inversion in the Laplace-Fourier domain: validation with marine and land seismic data.
SEG Technical Program Expanded Abstracts, pages 2476–2481, 2011.



P. Kaufl, A. Fichtner, and H. Igel.

Probabilistic full waveform inversion based on tectonic regionalization–development and application to the Australian upper mantle.
Geophysical Journal International, 193(1):437–451, January 2013.



L. Métivier, F Bretaudeau, R Brossier, S Operto, and J Virieux.

Full Waveform Inversion and the truncated Newton method : quantitative imaging of complex subsurface structures.
Geophysical Prospecting, in press, 2014.



L Métivier, R Brossier, Q Mérigot, E Oudet, and J Virieux.

Measuring the misfit between seismograms using an optimal transport distance: application to full waveform inversion.
Geophysical Supplements to the Monthly Notices of the Royal Astronomical Society, 205(1):345–377, 2016.



L Métivier, R Brossier, J Virieux, and S Operto.

Full waveform inversion and the truncated newton method.
SIAM Journal on Scientific . . . , pages 1–42, 2013.



S. Operto, Y. Gholami, V. Prieux, A. Ribodetti, R. Brossier, L. Metivier, and J. Virieux.

A guided tour of multiparameter full-waveform inversion with multicomponent data: From theory to practice.
The Leading Edge, 32(9):1040–1054, September 2013.



V. Prieux, R. Brossier, S. Operto, and J. Virieux.

Multiparameter full waveform inversion of multicomponent ocean-bottom-cable data from the Valhall field. Part 1: imaging compressional wave speed, density and attenuation.
Geophysical Journal International, 194(3):1640–1664, May 2013.



Dong Sun and WW Symes.

Waveform Inversion via Nonlinear Differential Semblance Optimization.
SEG Technical Program Expanded Abstracts, pages 1–5, 2012.



WW Symes.

The seismic reflection inverse problem.
Inverse problems, 25(12):123008, 2009.



Tristan van Leeuwen and Felix J Herrmann.

3D Frequency-domain seismic inversion with controlled sloppiness.
SIAM Journal of Scientific Computing, 36(5):S192–S217, 2014.



J. Virieux and S. Operto.

An overview of full-waveform inversion in exploration geophysics.
GEOPHYSICS, 74(6):WCC1–WCC26, November 2009.



Michael Warner and Lluís Guasch.

Adaptive waveform inversion: Theory.
Geophysics, 2016.



Pengliang Yang, Romain Brossier, Ludovic Mtivier, and Jean Virieux.

A review on the systematic formulation of 3-d multiparameter full waveform inversion in viscoelastic medium.
Geophysical Journal International, 207(1):129–149, 2016.



Fang Zhilong, Chia Ying Lee, Curt Da Silva, Felix Herrmann, and Tristan Van Leeuwen.

Uncertainty quantification for wavefield reconstruction inversion using a PDE-free semidefinite Hessian and randomize-then-optimize method, pages 1390–1394. 2016.



Hejun Zhu, Siwei Li, Sergey Fomel, Georg Stadler, and Omar Ghattas.

A bayesian approach to estimate uncertainty for full-waveform inversion using a priori information from depth migration. Geophysics, 81(5):R307–R323, 2016.